Confined 1*S* excitons, Landau transitions, and cavity mode coupling in GaAs microcavities

M. Opher-Lipson and E. Cohen
Solid State Institute, Technion-Israel Institute of Technology, Haifa 32000, Israel

A. Armitage, M. S. Skolnick, T. A. Fisher, and J. S. Roberts
Department of Physics, University of Sheffield, Sheffield S3 7RH, United Kingdom

L. N. Pfeiffer
Bell Laboratories, Lucent Technologies, Murray Hill, New Jersey 07974
(Received 18 August 1997; revised manuscript received 5 October 1998)

The reflection spectra of GaAs microcavities (MC) formed between GaAs/$Al_xGa_{1-x}As$ distributed Bragg reflectors were studied at $T=2$ K and under a magnetic field applied perpendicularly to the layers (z direction). Several MC's were studied, whose length $L_{MC}\sim\lambda_{exc}=223$ nm corresponds to the 1*S* exciton wavelength of bulk GaAs at $T=2$ K [$E(1S)=1.515$ eV]. The spectra show a large number of sharp lines either within the broad MC-confined photon band, when the MC mode overlaps the continuum absorption, or within the upper Rabi split band when the MC mode is near resonance with the lowest 1*S* exciton states. The energy and intensity of these sharp lines vary with increasing magnetic field ($0<B\leqslant 4$ T). For comparison, the reflection spectrum of a λ_{exc}-wide GaAs layer (cladded by 100 nm-wide $Al_{0.3}Ga_{0.7}As$ layers) was similarly studied. It did not show the magnetic-field-dependent features observed in the MC samples. It is shown that the reflection spectra of the MC samples are determined by the resonant coupling between three types of excitations: (a) 1*S* excitons with $k_z>0$ that are spatially confined in the λ_{exc}-wide MC, resulting in a quantization of their center of mass motion. (b) Landau transitions (magnetoexcitons) between electron and hole Landau levels with indices ranging up to $p=11$. (c) MC-confined photons. The reflection spectra are calculated by constructing transfer matrices that describe light propagation along the z direction (in the MC and in each layer of the distributed Bragg reflectors) and introducing an energy-dependent dielectric function for the GaAs layer, in the form of a Lorentzian oscillator response function for the 1*S* exciton and for each one of the magnetoexcitons. The 1*S* exciton center of mass quantization is introduced by including its k_z dispersion within the dielectric function and using Pekar's additional boundary condition. The calculated spectra fit reasonably well the experimental ones (in both energy and intensity). The fan diagrams show anticrossings between the spatially confined 1*S* exciton levels and the $p\geqslant 1$ magnetoexcitons, as they are tuned by the magnetic field. These anticrossings are observed experimentally only in the MC mode spectral range, as predicted by the model. Using the same model, the electronic excitations energy dependence on magnetic field is calculated for the λ_{exc}-wide GaAs layer confined between the $Al_{0.3}Ga_{0.7}As$ layers (namely without the distributed Bragg reflectors). No anticrossings are obtained. It is thus concluded that the spatially confined 1*S* exciton levels and the $p\geqslant 1$ magnetoexcitons are coupled via their interaction with the MC-confined photons.
[S0163-1829(99)03315-9]

I. INTRODUCTION

Semiconductor microcavities (MC) are currently intensively studied since their optical properties depend strongly on the coupling between the MC-confined photon mode and the electronic excitations.[1] So far, most of the investigations of semiconductor MC structures were focused on the coupling between the (two- or three-dimensional) exciton and the MC mode. The strongest observed interaction is that between quantum well excitons and confined photons.[2–4] In order to achieve it, the quantum wells (QW's) are embedded in the MC, formed between distributed Bragg reflectors (DBR), in a region of maximal radiation intensity. The interaction between the confined photon mode and the exciton is enhanced by tuning the exciton energy into resonance with the MC-mode energy. The resulting Rabi splitting is usually observed in reflection, transmission and photoluminescence spectra.

Recently, MC's consisting of a thin GaAs layer cladded on both sides by DBR's were studied by Chen, Tredicucci, and Bassani[5] and Tredicucci *et al.*[6,7] The MC widths (L_{MC}) were multiples of $\lambda_{exc}=hc/n_{GaAs}E(1S)$, the 1*S* excitonic transition wavelength. This results in a quantization of the 1*S* exciton center of mass motion. When the MC mode is resonant with the lowest energy excitonic transition, a Rabi splitting, and an enhancement of the excitonic fine structure are observed in the reflection spectra. These spectra were analyzed using a transfer-matrix formalism similar to the procedure used for QW's embedded in a MC.[5] A nonlocal dielectric function for the 1*S* exciton, including its k_z dispersion, was used in order to account for the quantization of the 1*S* exciton center of mass motion [along the MC normal (z) direction].

In this paper, we study the reflection spectra of λ_{exc}-wide GaAs MC's that are subjected to a magnetic field (B) applied perpendicularly to the MC plane. The field splits the electron

and hole continua into Landau levels and the interband transitions between them are the magnetoexcitons. The magnetoexcitons with Landau index $p \geqslant 1$ overlap the $1S$ exciton continuum spectral range. Magnetoexcitons were not observed in the reflection spectra of bulk GaAs.[8] However, they are clearly observed in the reflection and photoluminescence excitation spectra of the λ_{exc}-wide GaAs MC's studied here. We also studied the reflection spectra of a λ_{exc}-wide GaAs layer cladded by 100 nm $Al_{0.3}Ga_{0.7}As$ layers, and did not observe magnetoexcitons (with $p \geqslant 1$). Therefore, we utilize this MC-induced enhancement and the magnetoexcitons tunability with varying B in order to investigate the coupling between the following three types of excitations: (1) Spatially confined $1S$ exciton levels originating from high-k_z states (on the dispersion curve of the $1S$ exciton band). (2) Magnetoexcitons with a Landau index $p \geqslant 1$. (3) MC-confined photons. The degree of mixing between these three types of excitations depends upon the magnetic-field strength and on the MC mode-$1S$ exciton energy detuning. Consequently, the reflection spectra show a large number of spectral lines within the MC mode spectral range that vary in energy and intensity with increasing magnetic-field strength. Anticrossings between the electronic excitations are observed in the MC-mode spectral range.

The reflection spectra are analyzed by using a model based on transfer matrices that describe light propagation (along z in the λ_{exc}-wide GaAs layer and in each layer of the distributed Bragg reflectors) and an energy-dependent dielectric function having the form of a Lorentzian oscillator response function for the $1S$ exciton and each one of the magnetoexcitons.[5] The $1S$ exciton center of mass quantization is introduced by including its k_z dispersion relation within the dielectric function and using Pekar's additional boundary conditions.[7] This results in a series of reflection lines that are fitted to the experimental spectra (both energy and intensity). The model explains well the energy dependence of the sharp reflection lines on the magnetic-field strength and on the MC mode-$1S$ exciton energy detuning. The comparison between the experimental reflection spectra of the MC samples and the ''bare'' λ_{exc}-wide GaAs layer, and the model calculation lead to the main finding of this work: The two types of electronic excitations are strongly coupled to the MC photon modes. This induces a coupling between the electronic excitations that is manifest in anticrossings between the spatially confined $1S$ exciton levels and the $p \geqslant 1$ magnetoexcitons.

The paper is laid out as follows: In Sec. II we describe the experimental procedure and present our experimental results. Section III presents the theoretical model and the analysis of the experimental results. Section IV is a summary.

II. EXPERIMENTAL PROCEDURE AND RESULTS

The investigated MC structure consists of a GaAs layer whose width (L_{MC}) is of the order of the bulk exciton transition wavelength ($L_{MC} \sim \lambda_{exc} = 223$ nm at $T = 2$ K), located between two 12 periods distributed Bragg reflectors. Each reflector period consists of $Al_{0.1}Ga_{0.9}As$ and $Al_{0.4}Ga_{0.6}As$ layers with widths of 57 and 68 nm, respectively. The wafer containing the MC structure was grown by the metal-organic chemical vapor deposition method on a (001)-oriented GaAs substrate. We studied four different samples, all cut of the same wafer, [labeled (a)–(d)], with slightly different L_{MC}'s. We also studied a reference sample [labeled (e)] consisting of a λ_{exc}-wide GaAs layer cladded by a 100 nm $Al_{0.3}Ga_{0.7}As$ layer on each side and grown on a (001)-oriented GaAs.

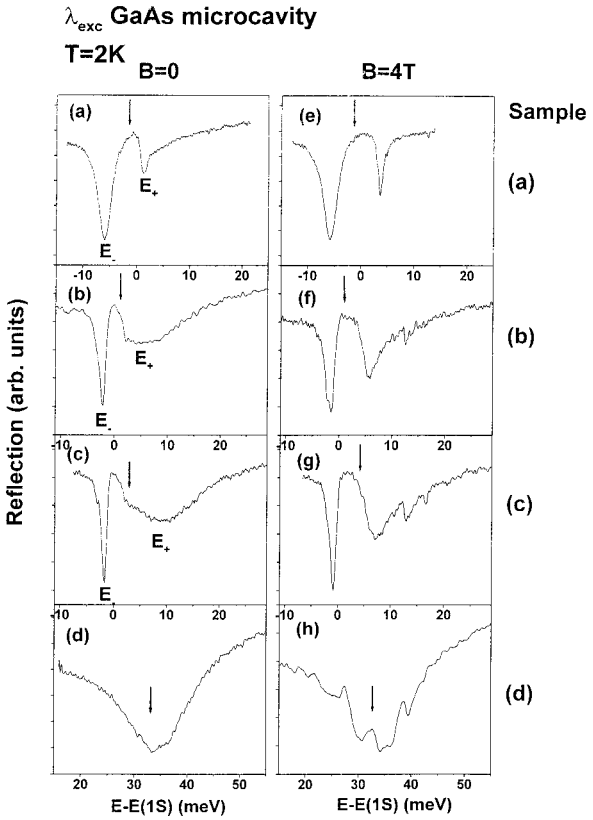

FIG. 1. Reflection spectra of the four samples [(a), (b), (c), and (d)] in the $1S$ exciton and MC-mode spectral range, for $B = 0$ (a)–(d) and $B = 4$ T (e)–(h). The down pointing arrows indicate the MC-mode energy (E_{cav}).

For the reflection measurements a tungsten filament lamp was used, and the incident and reflected beams were aligned perpendicularly to the sample surface ($\vec{k}_{photon} \| [001]$). The detection was done using a double spectrometer (with a spectral resolution of 0.05 meV). The samples were placed in a liquid-helium immersion dewar containing a superconducting magnet, and the magnetic field was perpendicular to the MC plane ($0 < B \leqslant 4$ T).

Figure 1 shows the reflection spectra of the four MC samples observed for $B = 0$ and $B = 4$ T. In samples (a), (b), and (c) the $1S$ exciton energy (set at 0) is close to resonance with the MC mode. Its energy, E_{cav}, is indicated by down pointing arrows. Therefore, a Rabi splitting (between the mixed E_+ and E_- modes) is observed.[7] In sample (d) the MC-mode band center is 33 meV above the $1S$ exciton energy, and it is very broad ($\Delta E = 8$ meV). Under an applied magnetic field, the upper band E_+ in the spectra of samples (a)–(c) and the broad MC mode band of sample (d) split into several narrow spectral lines [Figs. 1(e)–(h)]. Figure 2 shows the reflection spectra of samples (c) and (d) (solid lines) for several magnetic-field strengths. Figures 3 and 4 present the fan diagrams obtained by plotting the energy of each reflection minimum, (observed in spectra such as those shown in

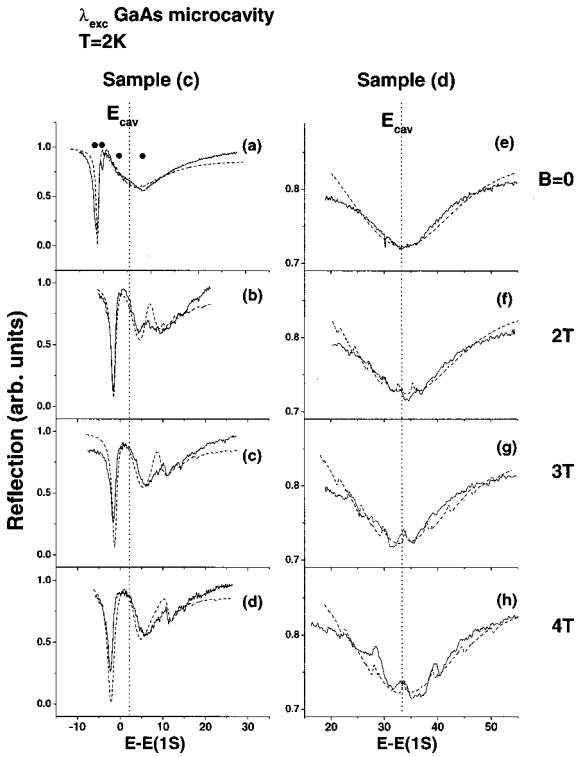

FIG. 2. Experimental reflection spectra of two MC samples (solid lines), measured under a magnetic field applied perpendicularly to the MC plane. The dots shown in (a) denote sharp features that correspond to spatially confined 1*S* exciton levels. The calculated spectra were obtained using the model discussed in Sec. III (dashed lines).

Fig. 2), as a function of magnetic-field strength for samples (c) and (d), respectively. The error bars correspond to the energy uncertainty in resolving the reflection minima.

We also measured the photoluminescence excitation spectra of samples (a)–(d) at different magnetic-field strengths and observed the same sharp lines at the same energies as observed in the reflection spectra.

Figure 5 shows the reflection spectrum of the reference sample (e) measured at $T=2$ K and $B=0$ (solid line). The observed fine structure is similar to that observed by Tredicucci *et al.*[6,7] and identified as due to the quantized levels of the 1*S* exciton center of mass motion. No sharp magnetoexcitons are observed in the reflectivity spectrum of this sample under an applied $B\leqslant 4$ T.

III. ANALYSIS

The reflection spectra are analyzed by using a model based on transfer matrices that describe light propagation (along *z* in the GaAs layer and in each layer of the distributed Bragg reflectors).[9] The $\lambda_{\rm exc}$-wide GaAs layer presents sharp optical transitions and thus, for its refraction index, we use an energy-dependent dielectric function that has the form of a Lorentzian oscillator response function for the 1*S* exciton and for each one of the $p\geqslant 1$ magnetoexcitons. We treat the 1*S* exciton separately, although it is the Landau transition with index $p=0$, since it has the strongest optical transition and a small, diamagnetic shift with increasing *B*.

The 1*S* exciton center of mass motion quantization is introduced by including its bulk dispersion relation within the dielectric function. The 1*S* exciton magnetic-field-dependent refractive index function is given by[10]

$$n_{\rm exc}^2(E,B)=n_{\rm GaAs}^2\left(1+\frac{\Gamma_0^{\rm exc}E_{\rm exc}(B)}{E_{\rm exc}^2(B)-E^2+i\Gamma^{\rm exc}E}\right). \qquad (1)$$

$n_{\rm GaAs}$ is the real part of the GaAs refractive index. Following Ref. 5, the 1*S* exciton oscillator strength is defined as $\Gamma_0^{\rm exc}E(1S)$, where $E(1S)=1.515$ eV is its energy at $k_z=0$ and $B=0$. $\Gamma^{\rm exc}$ is its damping. In order to account for the 1*S* exciton center of mass motion quantization in the $\lambda_{\rm exc}$-wide GaAs layer and for the exciton diamagnetic energy shift $\Delta(B)$, we introduce its dispersion relation:[11] $E_{\rm exc}(B,k_z)=E(1S)+\hbar^2k_z^2/2M_{\rm exc}^*+\Delta(B)$. Here, $M_{\rm exc}^*(=m_e^*+m_h^*)$ is the effective translational mass of the bulk heavy exciton. $\Delta(B)=aB+bB^2$, where $a=1.6\times10^{-4}$ eV/T and $b=6.2\times10^{-6}$ eV/T^2.[12] We obtained the *a* and *b* parameter values by measuring the 1*S* exciton lineshift with increasing *B* in the photoluminescence spectra of an ultrapure bulk GaAs sample.

The $p\geqslant 1$ magnetoexcitons contribution to the refractive index function is given by

$$n_{LL}^2(E,B)=n_{\rm GaAs}^2\left(\sum_p \frac{\Gamma_0^pE_p(B)}{E_p^2(B)-E^2-i\Gamma^pE}\right),\quad p=1,2\ldots. \qquad (2)$$

Here, E_p, $\Gamma_0^pE_p$, and Γ^p are the energy, oscillator strength and damping factor of the *p* magnetoexciton, respectively. $E_p(B)$ is approximately given by[12,13]

$$E_p(B)=E_{\rm gap}+\hbar\omega_c\left(p+\frac{1}{2}\right)-\frac{3}{8}\sqrt{\frac{E_B\hbar\omega_c}{(p+\frac{1}{2})}}. \qquad (3)$$

Here, $\hbar\omega_c=\hbar eB/m^*c$ is the exciton cyclotron energy (with $1/m^*=1/m_e^*+1/m_{hh}^*$) and $E_B[=E_{\rm gap}-E(1S)]$ is the binding energy of the 1*S* exciton in bulk GaAs (for $B=0$). Equation (3) is a good approximation for the magnetoexciton energies when $\hbar\omega_c(p+\frac{1}{2})\geqslant E_B$. It is thus expected to provide an accurate analysis of the fan diagram of sample (d) (Fig. 4) and a poorer description of those of samples (a)–(c) (such as that of Fig. 3). However, as will be discussed below, the main observation that can be made for all four MC structures is the anticrossings between magnetoexcitons with indices $p\geqslant 1$ and the quantized levels of the 1*S* exciton center of mass motion. The model calculations using Eq. (3), result in a small discrepancies from the observed fan diagram and reproduce well the level anticrossings.

The mixed exciton MC photon modes (exciton polaritons) of the MC structures are obtained by solving the equation

$$\frac{\hbar^2c^2k^2}{E^2(k)}=(n_{\rm exc}^2+n_{LL}^2). \qquad (4)$$

Consider first the $B=0$ case. In this case $n_{LL}=0$. We use Tredicucci, Chen, and Bassani procedure[7] in order to calculate the reflection spectra shown in Fig. 5 (dashed lines). Pekar's additional boundary conditions[5] are used, and the interband continuum absorption (for $E>E_{\rm gap}$) is introduced by replacing $n_{\rm GaAs}$ of Eq. (1) by

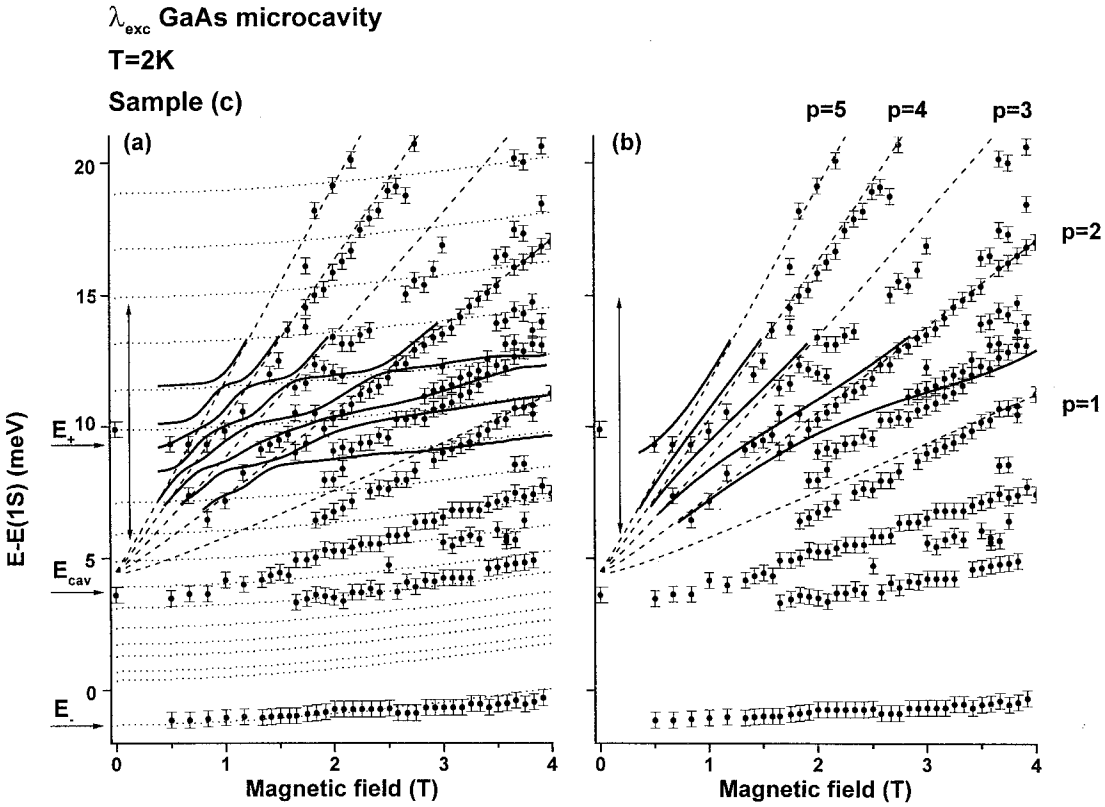

FIG. 3. (a) Experimental fan diagram obtained by plotting the energies of the reflection line minima of sample (c), (circles). For this sample $E_{\mathrm{cav}}=E(1S)+4$ meV. The calculated energies of the uncoupled, spatially confined $1S$ exciton levels and $p\geqslant 1$ magnetoexcitons are shown in dotted and dashed lines, respectively. The calculated energies of the mixed modes are shown in solid lines. (b) The same experimental fan diagram plotted with the energies of the reflection-line minima calculated by assuming an infinitely heavy $1S$ exciton translational mass.

$$n_{\mathrm{GaAs}}\left(1+i\frac{C}{E^2}(E-E_{\mathrm{gap}})^{1/2}\right)$$

with $C=1.2(\mathrm{eV})^{3/2}$ [Ref. 14]. The parameters used for the calculations are listed in Tables I and II. The calculated reflection spectra fit reasonably well the experimental ones. In samples (a), (b), and (c), the main reflection bands (the Rabi-split E_+ and E_- modes) are due to the MC-mode coupling to the lowest energy spatially confined $1S$ exciton levels. The higher energy quantized levels of the center of mass motion give rise to the weaker features. In fitting the $B=0$, reflection spectra of all four MC structures [Fig. 1(a)–(d)] we adjust L_{MC}, thereby tuning E_{cav} relative to $E(1S)$. It should be noted that the GaAs interband absorption must be introduced into the model in order to explain the large broadening of the E_+ band [Figs. 1(a)–(c)] and of the MC mode [Fig. 1(d)]. In the latter case, the relative intensity of the MC mode is smaller than that of the E_+ modes in the other MC samples since E_{cav} is far from resonance with the strongest $1S$ exciton transition.

Using the same model, we calculated the reflection of sample (e). Since the λ_{exc}-wide GaAs layer does not form a MC, the coupling between the $1S$ exciton and the resonant photons is much weaker than in the MC samples. The calculated spectrum (Fig. 5, dashed line) shows sharp features at energies that fit well those of the experimentally observed sharp lines. However, the relative intensities of the sharp lines are not well reproduced.

TABLE I. Parameters used for calculating the reflection spectra.

Definition	Value	Ref.
Γ_0^{exc} $1S$ exciton oscillator strength	1.325×10^{-5}	5
Γ^{exc} $1S$ exciton damping factor	0.1 meV	5
M^*_{exc} $1S$ exciton translational mass	$0.49m_0$	5
E_{gap} GaAs gap energy	1.5195 eV	5
$E(1S)$ GaAs exciton energy (at $k=0$ and $T=2$ K)	1.5151 eV	5
$\frac{h\omega_c}{B}$ GaAs cyclotron energy per unit B	1.38 meV/T	15
GaAs dielectric constant (at $T=2$ K)	12.44	14
AlAs dielectric constant (at $T=2$ K)	9.6	14

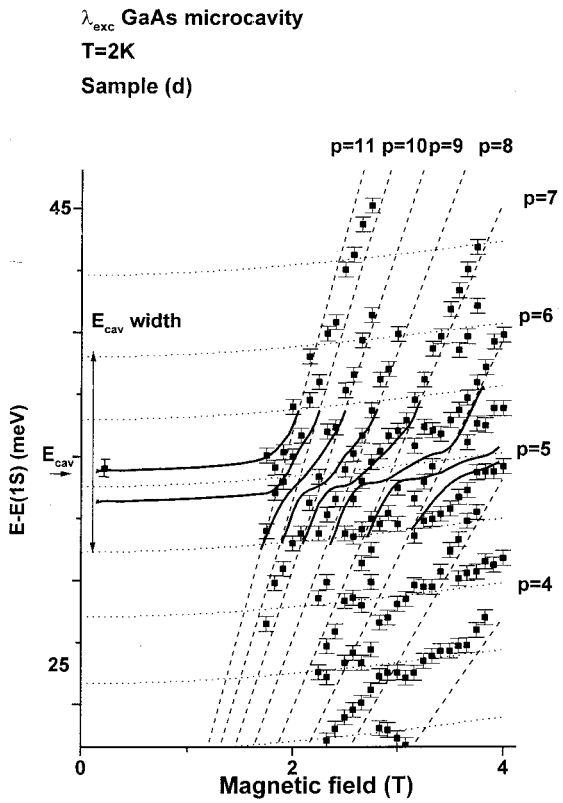

FIG. 4. Same plot as in Fig. 3(a), but for sample (d). In this case $E_{\mathrm{cav}}=E(1S)+33$ meV.

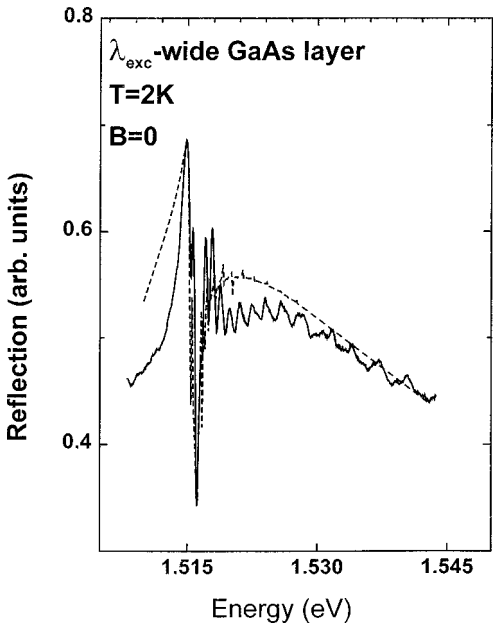

FIG. 5. Experimental and calculated reflection spectrum of sample (e) (solid and dashed lines, respectively).

We now repeat this calculation procedure for $B>0$ [using Eqs. (2)–(4)]. The Γ_p^0 and Γ_p parameters (for $p\geqslant 1$) are obtained from the spectra fitting and are listed in Table II. In the case of samples (b) and (c), the near resonance of the MC mode and the $1S$ exciton energy, enhances the low-index magnetoexcitons that are tuned into the MC mode spectral range by the magnetic field (cf. Figs. 2 and 3). In sample (a) $E_{\mathrm{cav}}<E(1S)$, and no magnetoexcitons with $p\geqslant 1$ are observed [Fig. 1(e)]. In sample (d), $E_{\mathrm{cav}}=E(1S)+33$ meV, the high-index magnetoexcitons and the high-energy-confined $1S$ exciton states that are tuned into the MC-mode spectral range are well fitted by the model calculations (cf. Figs. 2 and 4). Note that although the large interband absorption reduces the MC finesse,[4] it has the advantage that a large number of electronic transitions overlap the MC-mode band allowing us to fit the reflection spectra over a wide B range. We neglect the increase of the $1S$ exciton and $p\geqslant 1$ magnetoexcitons oscillator strengths with increasing magnetic field since for $2\leqslant B\leqslant 4$ T they change by only $\sim 10\%$.[2] Such an increase does not affect the fitting of the calculated spectra to the experimental ones. Also, the magnetoexcitons k_z dispersion is not included in the model [Eq. (3)]. It would introduce an energy correction to the magnetoexciton polaritons that is much smaller than the experimental error bars of Figs. 3 and 4. The calculated reflection spectra [shown by dashed lines in Figs. 2(a)–2(d) and 2(e)–2(h)] fit well both the energy and the intensity of the experimentally observed sharp reflection lines.

In Fig. 3(a) we plot the energy of the sharp line minima as obtained from the calculated reflection spectra of sample (c) as a function of B, (solid lines). The energies of the uncoupled, spatially confined $1S$ exciton levels and those of the Landau transitions ($p\geqslant 1$) are also plotted (dotted and dashed lines, respectively). The energies of the MC mode (E_{cav}), $1S$ exciton [$E(1S)$] and the mixed modes (E_+ and E_-) at $B=0$ are indicated. At energies $E>E_+$, namely, $E\geqslant E(1S)+15$ meV, and for $B>2$ T, the mixing between these three types of excitations does not affect their energy but enhances the fine-line intensities. Then, the calculated uncoupled Landau transitions energies fit the experimental

TABLE II. Fitting parameters used for calculating the reflection spectra.

Definition	Value
MC-mode energy: Sample (a)	$E(1S)-(1.0\pm 0.2)$ meV
Sample (b)	$E(1S)+(1.0\pm 0.2)$ meV
Sample (c)	$E(1S)+(4.0\pm 0.2)$ meV
Sample (d)	$E(1S)+(33.0\pm 0.2)$ meV
$\Gamma_0^1 p=1$ Landau transition oscillator strength	$(0.20\pm 0.05)\Gamma_0^{\mathrm{exc}}$
Γ_0^p $2\leqslant p\leqslant 11$ Landau transition oscillator strength	$(0.05\pm 0.01)\Gamma_0^{\mathrm{exc}}$
$\Gamma^1 p=1$ Landau transition damping factor	$(1.0\pm 0.2)\Gamma^{\mathrm{exc}}$
Γ^p $2\leqslant p\leqslant 11$ Landau transition damping factor	$(5\pm 1)\Gamma^{\mathrm{exc}}$

data. Within the E_+ spectral region, namely, $E \geqslant E(1S) + 9$ meV, mixing is induced between the spatially confined $1S$ exciton center of mass levels and the magnetoexcitons. For example, anticrossing between the $p=2$ Landau level and a spatially confined $1S$ exciton level at $E=E(1S)+11$ meV is observed around $B=2.5$ T. A similar anticrossing between the latter with the $p=3$ Landau transition is obtained around $B=1.7$ T, and so on.

In order to show the importance of the $1S$ exciton center of mass quantization in explaining the experimental data, we plot in Fig. 3(b) the same experimental data as in Fig. 3(a) and the calculated mixed modes energies, assuming an infinitely heavy $1S$ exciton translational mass, $M^*_{\rm exc} \rightarrow \infty$ (i.e., without the quantization of the $1S$ exciton center of mass motion). Then, for $E > E_+$, the experimental energies of the sharp reflection lines generally follow the calculated $p=2,3,4$ magnetoexciton energies. However, within the E_+ mode width the experimental data can be fitted only when the $1S$ exciton center of mass motion quantization and the magnetoexcitons are introduced.

In Fig. 4, we plot the calculated reflection line minima of sample (d) and the experimental fan diagram in the MC mode spectral region $[E_{\rm cav} \sim E(1S)+33\,{\rm meV}]$. A large number of magnetoexcitons ($4 \leqslant p \leqslant 11$) and high-energy transitions of the quantized $1S$ exciton center of mass motion appear in this spectral range and the mixing between them is evident.

We now discuss the physical mechanism that leads to these level anticrossings. The spatially confined excitons originate from the high-k_z states of the $1S$ exciton band. Under a magnetic field applied perpendicularly to the QW plane, the $1S$ exciton band consists mainly of the $p=0$ electron and hole Landau levels and will show a diamagnetic shift for all k_z values. Calculations of the energy states of a two-dimensional exciton under an applied magnetic-field show[12,15] that the $p=0$ exciton wave function is orthogonal to those of the high-p states. This was verified experimentally[8] for the case of bulk GaAs, where a diamagnetic shift was observed for the $1S$ exciton even for $B \sim 12$ T. From this we conclude that for a thin GaAs layer, the magnetic field does not admix magnetoexcitons with high Landau indices with those originating from the lowest ($p=0$) magnetoexciton band.

In order to further examine the essential role of the coupling between the electronic excitations and the MC mode, we also calculated the spectra (as a function of B) for the ''bare'' $\lambda_{\rm exc}$-wide GaAs layer [sample (e)], using the same material parameters as for the other samples. The fan diagram was obtained by repeating the calculations for B increasing with $\Delta B = 0.02$ T steps. In Fig. 6, we plot the energies of all the sharp minima that appear in the calculated reflection spectra. It is clear that no anticrossing between magnetoexcitons and the spatially confined $1S$ exciton levels is obtained. Note that the energies corresponding to the minima in the measured reflection spectra for $B=0$ are also shown (squares) and they fit well the calculated energies. As mentioned in Sec. II, no magnetoexcitons are observed in this case. This results from their small oscillator strengths.

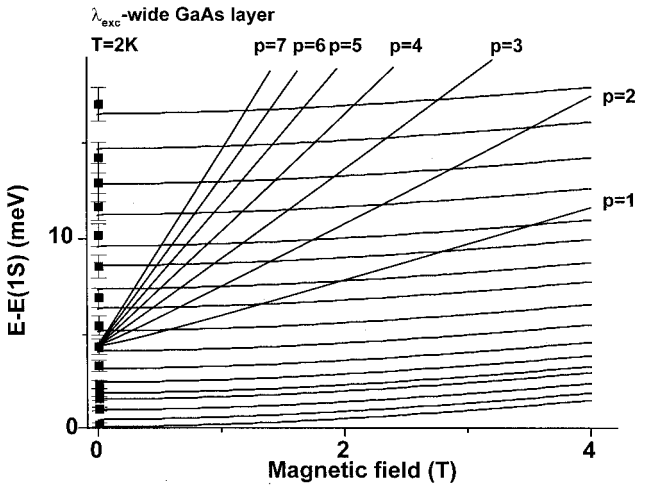

FIG. 6. Fan diagram obtained by plotting the calculated energies of the reflection-line minima of sample (e), as a function of magnetic field. The energies corresponding to the minima in the measured reflection spectra at $B=0$, are also shown (squares).

IV. SUMMARY

We presented a detailed spectroscopic study of the magnetic-field effect on the coupled exciton-confined photon modes in $\lambda_{\rm exc}$-wide GaAs MC's. The electronic excitations of the GaAs layer (that forms the MC) are of two types: (a) Spatially confined $1S$ excitons. These appear as quantized levels of the exciton center of mass motion, and they show a diamagnetic energy shift even for high energies on the k_z dispersion relation. (b) Magnetoexcitons that are formed of electrons and holes in Landau levels with indices $p \geqslant 1$. These electronic excitations interact strongly with the MC confined photons when they are at resonance. Consequently, the MC samples have reflection spectra under an applied magnetic field that are rich in sharp lines with a B-dependent energy and intensity. The fan diagrams extracted of these reflection spectra show a complex B-dependence: Within the bandwidth of the MC mode there are anticrossings between the spatially confined $1S$ exciton levels and the magnetoexcitons with Landau indices $p \geqslant 1$. Outside the MC-mode bandwidth, the sharp reflection lines follow either the confined $1S$ exciton or the high-p magnetoexciton B dependence. For comparison, we also measured the reflection spectra of a $\lambda_{\rm exc}$-wide GaAs layer cladded by $Al_{0.3}Ga_{0.7}As$ layers under an applied magnetic field, and no sharp Landau transitions were observed for $E > E_{\rm gap}$.

We used a model based on transfer matrices that describe light propagation (in the $\lambda_{\rm exc}$-wide GaAs MC and in each layer of the distributed Bragg reflectors) and an energy-dependent dielectric function that assumes a Lorentzian oscillator response function for the exciton and for each one of the Landau transitions. The $1S$ exciton center of mass motion quantization is introduced by including its bulk dispersion relation within the dielectric function. The calculated spectra fit well the experimental ones. Using this model we identify the sharp lines as transitions between the mixed electronic excitations within the MC-mode bandwidth. The model explains well the level anticrossings

with increasing magnetic field strength. The main conclusion that is drawn from the analysis of the observed spectra (and fan diagrams) is that the anticrossings between the electronic excitations result from their interaction with the MC mode. In the MC-mode spectral range, each one of the electronic excitations interacts strongly with the MC mode.

ACKNOWLEDGMENTS

The work at the Technion was done in the Barbara and Norman Seiden Center for Advanced Optoelectronics and was supported by the U.S.–Israel Binational Science Foundation (BSF), Jerusalem.

[1] For review articles see *Confined Electrons and Photons: New Physics and Applications*, edited by E. Burstein and C. Weisbuch (Plenum, New York, 1995).
[2] T. A. Fisher, A. M. Afshar, M. S. Skolnick, and D. M. Whittaker, Phys. Rev. B **53**, 10 469 (1996).
[3] J. D. Berger, O. Lyngnes, H. M. Gibbs, G. Khitrova, T. R. Nelson, E. K. Lindmark, A. V. Kavokin, M. A. Kaliteevski, and V. V. Zapasski, Phys. Rev. B **54**, 1975 (1996).
[4] J. Tignon, P. Voisin, C. Delalande, M. Voos, R. Houdre, U. Oesterle, and R. P. Stanley, Phys. Rev. Lett. **74**, 3967 (1995).
[5] Y. Chen, A. Tredicucci, and F. Bassani, Phys. Rev. B **52**, 1800 (1996).
[6] A. Tredicucci, Y. Chen, V. Pellegrini, M. Borger, L. Sorba, G. Beltram, and F. Bassani, Phys. Rev. Lett. **75**, 3906 (1995).
[7] A. Tredicucci, Y. Chen, and F. Bassani, Phys. Rev. B **47**, 10 348 (1993).
[8] D. Bimberg, Adv. Solid State Phys. **17**, 195 (1977).
[9] M. Opher-Lipson, E. Cohen, and L. N. Pfeiffer, Phys. Rev. B **55**, 13 778 (1997).
[10] E. L. Ivchenko and I. Nesvizhskii, Fiz. Tverd. Tela St. Petersburg **36**, 2118 (1994) [Phys. Solid State **36**, 1156 (1994)].
[11] J. Kusano, Y. Segawa, M. Mihara, A. Aoyagi, and S. Namba, Solid State Commun. **72**, 215 (1989).
[12] O. Akimoto and H. Hasegawa, J. Phys. Soc. Jpn. **22**, 181 (1967).
[13] D. C. Rogers, J. Singleton, R. J. Nicholas, C. T. Foxon, and K. Woodbridge, Phys. Rev. B **34**, 4002 (1986).
[14] S. Adachi, *GaAs and Related Materials* (World Scientific, Singapore, 1994), Chap. XI, p. 359.
[15] D. Heiman, Semicond. Semimet. **36**, 2 (1992).